Magnetic Materials

DOI: 10.1002/ange.200604452

Coexistence of Ferroelectricity and Ferromagnetism in a Rubidium Manganese Hexacyanoferrate**

Shin-ichi Ohkoshi, Hiroko Tokoro, Tomoyuki Matsuda, Hitomi Takahashi, Hiroshi Irie, and Kazuhito Hashimoto*

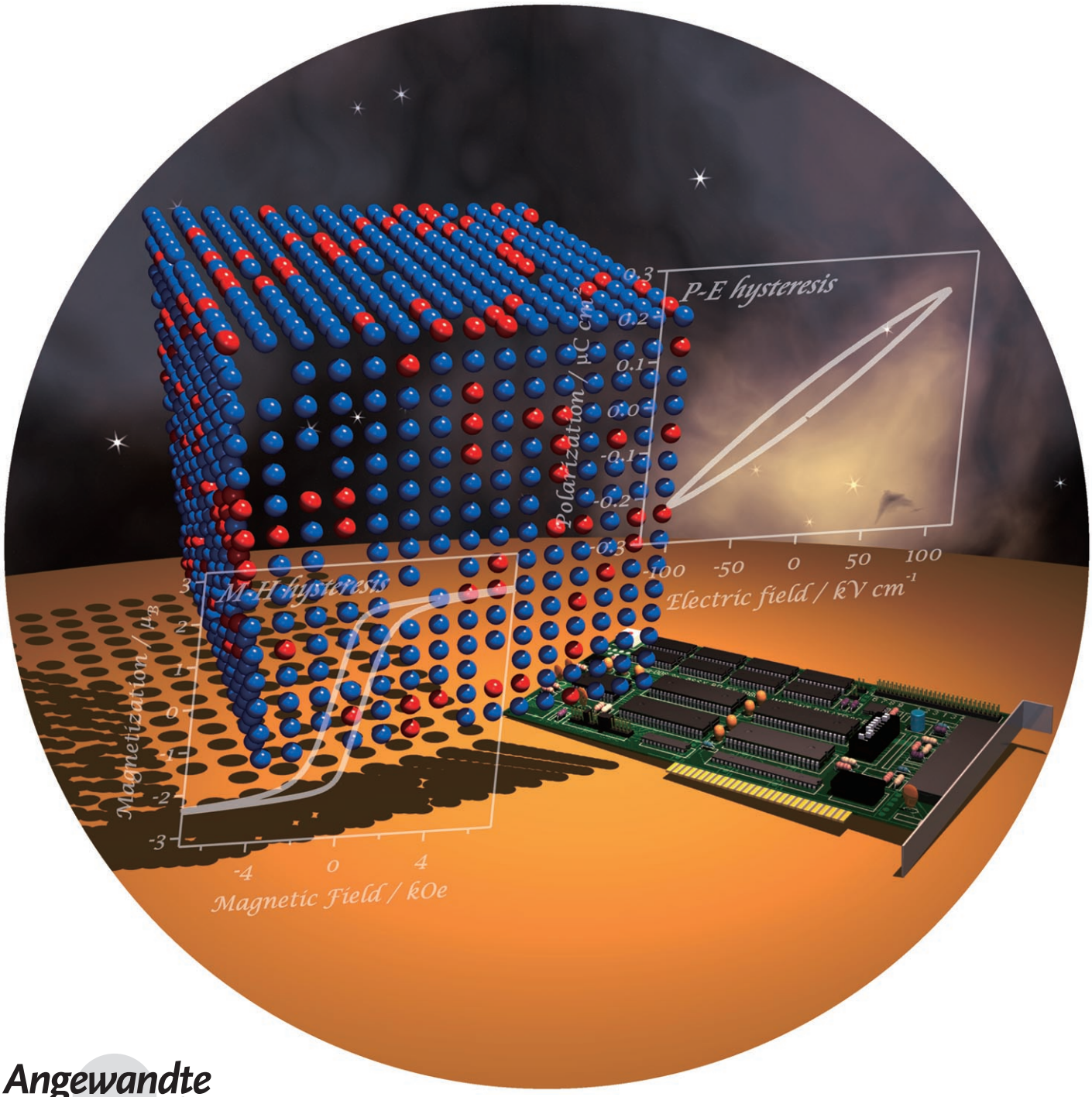

A ferroelectric ferromagnet, which is one of the multiferroics, has received significant attention because it is expected to exhibit various functionalities owing to the interaction between the electric polarization and magnetic polarization.[1] The realization of a ferroelectric ferromagnet is one of the targets in the field of coordination polymers. To achieve this objective, we have focused on hexacyanometalate-based materials,[2–4] which are composed of transition-metal ions and cyano groups, since organic cyanopolymers are known to show ferroelectricity of the order–disorder type.[5] Hexacyanometalate-based materials are reported to show the ferromagnetism with a high Curie temperature[2] and unique functionalities.[3,4] A rubidium manganese hexacyanoferrate is an attractive material because it shows a charge-transfer phase transition and a ferromagnetic phase transition.[6] If a structural distortion is induced in this polymer, it may show ferroelectricity. In this work, we observed the coexistence of ferroelectricity and ferromagnetism in $Rb^{I}_{0.82}Mn^{II}_{0.20}Mn^{III}_{0.80}[Fe^{II}(CN)_6]_{0.80}[Fe^{III}(CN)_6]_{0.14}\cdot H_2O$. The ferroelectricity is due to the mixing of Fe^{II}, Fe^{III}, Fe vacancies, Mn^{II}, and Jahn–Teller-distorted Mn^{III} centers, and the ferromagnetism is mainly caused by a parallel ordering of the magnetic spins on the Mn^{III} centers.

The target material, $Rb_{0.82}Mn[Fe(CN)_6]_{0.94}\cdot H_2O$, shows a charge-transfer phase transition from high-temperature (HT) phase to low-temperature (LT) phase with the phase-transition temperatures of 184 K ($T_{1/2\downarrow}$) and 276 K ($T_{1/2\uparrow}$) in the cooling and warming process, respectively (see Figure S1 in the Supporting Information). In the IR spectra, the intensity of the CN stretching peak (Fe^{III}-CN-Mn^{II}) at $\tilde{\nu} = 2152\ cm^{-1}$ decreases as the temperature decreases, and a new broad CN peak (Fe^{II}-CN-Mn^{III}) appears near 2095 cm^{-1}. By reference to the ratio between Fe^{III}-CN-Mn^{II} and Fe^{II}-CN-Mn^{III} intensities, the valence states of HT and LT phases are determined to be $Rb^{I}_{0.82}Mn^{II}[Fe^{III}(CN)_6]_{0.94}\cdot H_2O$ and $Rb^{I}_{0.82}Mn^{II}_{0.20}Mn^{III}_{0.80}[Fe^{II}(CN)_6]_{0.80}[Fe^{III}(CN)_6]_{0.14}\cdot H_2O$, respectively (Figure S2 in the Supporting Information). Variable-temperature XRD measurements indicate that the crystal structures of the HT and LT phases are cubic (space group $F\bar{4}3m$, $a = 10.567(8)$ Å) and orthorhombic (space group $F222$, $a = 10.18(4)$, $b = 10.04(5)$, $c = 10.53(4)$ Å), respectively (Figure S3 in the Supporting Information). The magnetization versus temperature plots of the LT phase show ferromagnetism with a Curie temperature of 11 K (inset of Figure 1). The magnetization versus external magnetic field plots show a saturation-magnetization value of 3.4 μ_B (Figure S4 in the Supporting Information), which is mainly due to the magnetization for the parallel ordering of Mn^{III}, and a magnetic hysteresis loop with a coercive field of 800 Oe is observed at 2 K (Figure 1). The mechanism of the Mn^{III}–Mn^{III} ferromagnetic coupling is understood by a valence-delocalization mechanism.[7]

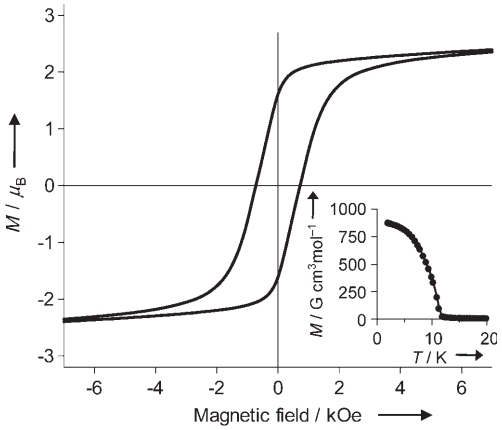

Figure 1. *M–H* hysteresis loop of $Rb^{I}_{0.82}Mn^{II}_{0.20}Mn^{III}_{0.80}[Fe^{II}(CN)_6]_{0.80}[Fe^{III}(CN)_6]_{0.14}\cdot H_2O$ at 2 K. Inset: magnetization versus temperature plots under an external field of 10 Oe.

Figure 2a shows the polarization (P) versus electric field (E) plots for the LT phase at 77 K when applying a field up to $\pm 100\ kV\,cm^{-1}$. The resulting curve shows an electric hysteresis loop with a remnant electric polarization (P_r) of 0.041 $\mu C\,cm^{-2}$ and an electric coercive field (E_c) of 17.5 $kV\,cm^{-1}$. Because the leakage current is extremely low (less than $10^{-10}\ A\,cm^{-2}$, measurement limitation is $10^{-9}\ A\,cm^{-2}$) under the employed conditions (Figure S5 in the Supporting Information), the observed hysteresis loop is clearly due to ferroelectricity. Figure 2b and Figure 2c show the P_r versus E and the E_c versus E plots at 77 K, respectively. The P_r and E_c values are nearly zero in a weak electric field, but the values increase when applying a strong electric field, thus suggesting that the observed P–E hysteresis loop is in the process of increasing the P_r and E_c values. The temperature dependences of the P_r and E_c values show that these values are nearly constant in the temperature region of 77–160 K (Figure S6 in the Supporting Information). Above 160 K, the leakage current appears under the strong electric field (Figure S7 in the Supporting Information). In the dielectric constant (ε) versus temperature plots of the LT phase, the increase of the ε value is observed above 200 K in the warming process, thus suggesting that a ferroelectric phase

[*] Prof. Dr. S. Ohkoshi, Dr. H. Tokoro, T. Matsuda, H. Takahashi
Department of Chemistry
School of Science
The University of Tokyo
7-3-1 Hongo, Bunkyo-ku, Tokyo 113-0033 (Japan)
E-mail: ohkoshi@chem.s.u-tokyo.ac.jp
Prof. Dr. S. Ohkoshi, Dr. H. Tokoro, T. Matsuda, H. Takahashi, Dr. H. Irie, Prof. Dr. K. Hashimoto
Department of Applied Chemistry
School of Engineering
The University of Tokyo
7-3-1 Hongo, Bunkyo-ku, Tokyo 113-8656 (Japan)

[**] We are grateful to Mr. A. Takashima (Ya-Man Co.) for helpful discussion on measurement. This research is supported in part by a Grant-in-Aid for 21st Century COE Programs for Frontiers in Fundamental Chemistry and for Human-Friendly Materials based on Chemistry, a Grant-in-Aid for Scientific Research from the Ministry of Education, Culture, Sports, Science and Technology of Japan, JSPS and RFBR under the Japan–Russia Research Cooperative Program, the Precursory Research for Embryonic Science and Technology program, Japan Science and Technology Corporation, and Yamada Science Foundation.

Supporting information for this article is available on the WWW under http://www.angewandte.org or from the author.

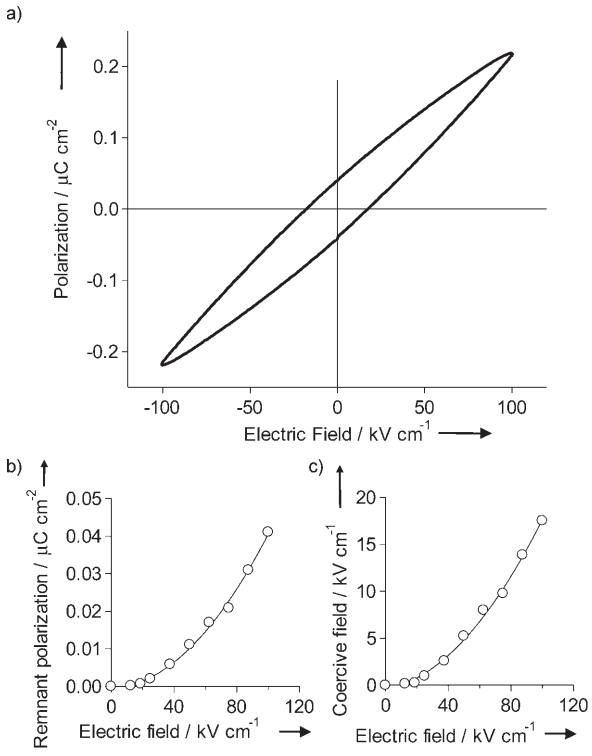

Figure 2. a) Polarization versus electric field curve (*P*–*E* hysteresis loop) of $Rb^{I}_{0.82}Mn^{II}_{0.20}Mn^{III}_{0.80}[Fe^{II}(CN)_6]_{0.80}[Fe^{III}(CN)_6]_{0.14}\cdot H_2O$ at 77 K. b) Remnant polarization (P_r) versus *E* plot. c) Electric coercive field (E_c) versus *E* plot at 77 K.

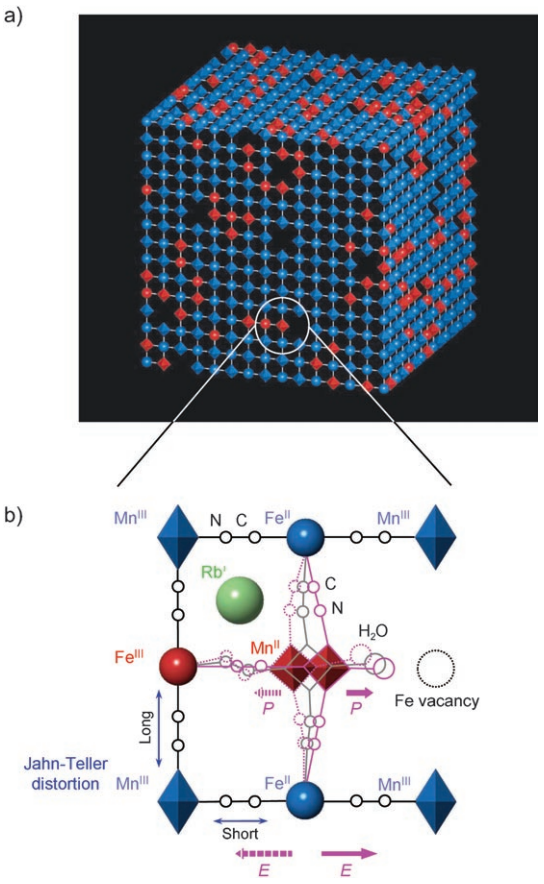

Figure 3. a) Schematic illustration of $Rb^{I}_{0.82}Mn^{II}_{0.20}Mn^{III}_{0.80}[Fe^{II}(CN)_6]_{0.80}[Fe^{III}(CN)_6]_{0.14}\cdot H_2O$. The positions of Mn^{II}/Fe^{III} sites, Mn^{III}/Fe^{II} sites, and Fe vacancies were chosen by computing with random numbers. b) Schematic illustration of a possible mechanism of ferroelectricity.

transition occurs (Figure S8 in the Supporting Information). Figure 3a schematically illustrates $Rb^{I}_{0.82}Mn^{II}_{0.20}Mn^{III}_{0.80}[Fe^{II}(CN)_6]_{0.80}[Fe^{III}(CN)_6]_{0.14}\cdot H_2O$, in which the positions of the Mn^{II}, Mn^{III}, Fe^{II}, Fe^{III}, and Fe vacancies are chosen by computing with random numbers. In the analogous compounds $Rb^{I}_{0.94}Mn^{II}_{0.02}Mn^{III}_{0.98}[Fe^{III}(CN)_6]_{0.98}\cdot 0.4\,H_2O$, $Rb^{I}_{0.28}Mn^{II}[Fe^{III}(CN)_6]_{0.76}\cdot 3.6\,H_2O$, and $K^{I}_{0.10}Mn^{II}[Fe^{III}(CN)_6]_{0.70}\cdot 4.5\,H_2O$ (Figure S9 in the Supporting Information), the *P*–*E* hysteresis loops are much smaller than that of the compound presented here (Figure S10 in the Supporting Information). Hence, the ferroelectricity of the compound reported here is related to mixing of Fe^{II}, Fe^{III}, Fe vacancy, Mn^{II}, and Jahn–Teller-distorted Mn^{III}. One of the possible mechanisms of the ferroelectricity is as follows. In $Rb^{I}_{0.82}Mn^{II}_{0.20}Mn^{III}_{0.80}[Fe^{II}(CN)_6]_{0.80}[Fe^{III}(CN)_6]_{0.14}\cdot H_2O$, a multimetallic Prussian blue analogue, a local electric dipole moment is created because of a Fe vacancy. In addition, the difference in ionic radii among four metal ions and Mn^{III} Jahn–Teller distortion enhance the local structural distortion, for example, the deviation of M-CN-M′ linkages from a 180° configuration.[6c] Probably, in such a deviated structure, polarization will be induced by the applied electric field, and the polarization can be held by the structural flexibility of the cyano-bridged 3D network. Along this line, we illustrate the ferroelectricity as shown in Figure 3b.

In this work, we observed ferroelectric ferromagnetism with a rubidium manganese hexacyanoferrate. This is one of the first examples of a ferroelectric ferromagnet in coordination polymers, although ferroelectric coordination polymers[5,8] or ferromagnetic coordination polymers have been reported. In a ferroelectric ferromagnet, the magnetoelectric (ME) effect[1] and a nonlinear magneto-optical effect such as magnetization-induced second-harmonic generation (MSHG)[9] are expected to be observed. We are now investigating these effects in this system.

Experimental Section

$Rb_{0.82}Mn[Fe(CN)_6]_{0.94}\cdot H_2O$: An aqueous solution of $MnCl_2$ (0.1 mol dm^{-3}) was treated with a mixed aqueous solution of RbCl (0.3 mol dm^{-3}) and $K_3[Fe(CN)_6]$ (0.1 mol dm^{-3}) to yield a precipitate. The precipitate was filtered and dried, and a powdered sample was obtained. Elemental analyses, which were confirmed by inductively coupled plasma mass spectroscopy and standard microanalytical methods, showed that the formula was $Rb_{0.82}Mn[Fe(CN)_6]_{0.94}\cdot H_2O$. Elemental analysis (%) calcd for $Rb_{0.82}Mn[Fe(CN)_6]_{0.94}\cdot H_2O$: Rb 20.48, Mn 16.05, Fe 15.34, C 19.79, N 23.08; found: Rb 20.42, Mn 16.13, Fe 15.31, C 19.61, N 23.06. The C-N stretching vibration was observed at $\tilde{\nu} = 2152\ cm^{-1}$ in the infrared spectra. The sample used to measure the ferroelectric property was prepared by the following process. The powdered compound was pressed uniaxially at 70 MPa, which produced a disk pellet with a 13-mm diameter and a 0.40-mm thickness. The obtained pellet was deposited with Pt on a surface and electroded with Au conductive paste. Then, Cu wire was used as electric terminals and sealed with an epoxy resin. The electric

polarization (P) versus the applied electric field (E) plots and the leakage current versus E plots were measured at 77 K by using an electric polarization hysteresis meter (TF Analyzer 1000, aixACCT). As reference experiments, we measured P versus E plots of SiO_2 glass, $Mn[Cr(CN)_6]_{2/3}\cdot 5H_2O$,[2a,10] $Co[Cr(CN)_6]_{2/3}\cdot 5H_2O$,[2a,3b,11] and $CsCo[Cr(CN)_6]\cdot 0.5H_2O$,[2a,11] and found that the reference samples show straight lines without hysteresis loops (Figure S11 in the Supporting Information).

Received: October 30, 2006
Published online: March 7, 2007

Keywords: coordination polymers · cyanides · ferromagnets · iron · manganese

[1] a) W. Eerenstein, N. D. Mathur, J. F. Scott, *Nature* **2006**, *442*, 759 – 765; b) G. A. Smolenskii, I. E. Chupis, *Sov. Phys. Usp.* **1982**, *25*, 475 – 493; c) J. Wang, J. B. Neaton, H. Zheng, V. Nagarajan, S. B. Ogale, B. Liu, D. Viehland, V. Vaithyanathan, D. G. Schlom, U. V. Waghmare, N. A. Spaldin, K. M. Rabe, M. Wuttig, R. Ramesh, *Science* **2003**, *299*, 1719 – 1722; d) J. Hemberger, P. Lunkenheimer, R. Fichtl, H.-A. Krug von Nidda, V. Tsurkan, A. Loidl, *Nature* **2005**, *434*, 364 – 367; e) Y. Tokura, *Science* **2006**, *312*, 1481 – 1482; f) N. A. Spaldin, M. Fiebig, *Science* **2005**, *309*, 391 – 392; g) T. Kanai, S. Ohkoshi, A. Nakajima, T. Watanabe, K. Hashimoto, *Adv. Mater.* **2001**, *13*, 487 – 490.

[2] a) M. Verdaguer, A. Bleuzen, V. Marvaud, J. Vaissermann, M. Seuleiman, C. Desplanches, A. Scuiller, C. Train, R. Garde, G. Gelly, C. Lomenech, I. Rosenman, P. Veillet, C. Cartier, F. Villain, *Coord. Chem. Rev.* **1999**, *190–192*, 1023 – 1047; b) S. Ferlay, T. Mallah, R. Ouahès, P. Veillet, M. Verdaguer, *Nature* **1995**, *378*, 701 – 703; c) S. M. Holmes, G. S. Girolami, *J. Am. Chem. Soc.* **1999**, *121*, 5593 – 5594; d) Ø. Hatlevik, W. E. Buschmann, J. Zhang, J. L. Manson, J. S. Miller, *Adv. Mater.* **1999**, *11*, 914 – 918; e) S. Ohkoshi, M. Mizuno, G. J. Hung, K. Hashimoto, *J. Phys. Chem. B* **2000**, *104*, 9365 – 9367.

[3] a) J. S. Miller, *MRS Bull.* **2000**, *25*, 60 – 64; b) S. Ohkoshi, K. Arai, Y. Sato, K. Hashimoto, *Nat. Mater.* **2004**, *3*, 857 – 861; c) S. Ohkoshi, K. Hashimoto, *J. Photochem. Photobiol. C* **2001**, *2*, 71 – 88; d) O. Sato, T. Iyoda, A. Fujishima, K. Hashimoto, *Science* **1996**, *272*, 704 – 705; e) D. A. Pejaković, J. L. Manson, J. S. Miller, A. J. Epstein, *Phys. Rev. Lett.* **2000**, *85*, 1994 – 1997; f) M. Kamiya, M. Hanawa, Y. Moritomo, Y. Isobe, J. Tateishi, K. Kato, A. Nakamura, *Phys. Rev. B* **2004**, *69*, 052102; g) F. Varret, A. Goujon, K. Boukheddaden, M. Noguès, A. Bleuzen, M. Verdaguer, *Mol. Cryst. Liq. Cryst.* **2002**, *379*, 333 – 340; h) A. Dei, *Angew. Chem.* **2005**, *117*, 1184 – 1187; *Angew. Chem. Int. Ed.* **2005**, *44*, 1160 – 1163; i) E. Coronado, M. C. Giménez-López, G. Levchenko, F. M. Romero, V. García-Baonza, A. Milner, M. Paz-Pasternak, *J. Am. Chem. Soc.* **2005**, *127*, 4580 – 4581; j) M. Nishino, K. Boukheddaden, S. Miyashita, F. Varret, *Phys. Rev. B* **2005**, *72*, 064452.

[4] a) S. Margadonna, K. Prassides, A. N. Fitch, *J. Am. Chem. Soc.* **2004**, *126*, 15390 – 15391; b) S. S. Kaye, J. R. Long, *J. Am. Chem. Soc.* **2005**, *127*, 6506 – 6507; c) A. L. Goodwin, K. W. Chapman, C. J. Kepert, *J. Am. Chem. Soc.* **2005**, *127*, 17980 – 17981.

[5] a) H. S. Nalwa (Ed.), *Ferroelectric Polymers: Chemistry, Physics, and Applications*, Marcel Dekker, New York, **1995**; b) S. Waku, H. Hirabayashi, H. Toyoda, H. Iwasaki, *J. Phys. Soc. Jpn.* **1959**, *14*, 973 – 974.

[6] a) H. Tokoro, S. Ohkoshi, T. Matsuda, K. Hashimoto, *Inorg. Chem.* **2004**, *43*, 5231 – 5236; b) Y. Moritomo, A. Kuriki, K. Ohoyama, H. Tokoro, S. Ohkoshi, K. Hashimoto, N. Hamada, *J. Phys. Soc. Jpn.* **2003**, *72*, 456 – 457; c) Y. Moritomo, M. Hanawa, Y. Ohishi, K. Kato, M. Takata, A. Kuriki, E. Nishibori, M. Sakata, S. Ohkoshi, H. Tokoro, K. Hashimoto, *Phys. Rev. B* **2003**, *68*, 144106; d) S. Margadonna, K. Prassides, A. N. Fitch, *Angew. Chem.* **2004**, *116*, 6476 – 6479; *Angew. Chem. Int. Ed.* **2004**, *43*, 6316 – 6319.

[7] Neutron powder experiment reveals that Mn^{III}–Mn^{III} ferromagnetic coupling exists on the LT phase; Y. Moritomo, A. Kuriki, K. Ohoyama, H. Tokoro, S. Ohkoshi, K. Hashimoto, N. Hamada, *J. Phys. Soc. Jpn.* **2003**, *72*, 456 – 457.

[8] a) P. Espinet, J. Etxeberria, M. Marcos, J. Perez, A. Remón, J. L. Serrano, *Angew. Chem.* **1989**, *101*, 1076 – 1078; *Angew. Chem. Int. Ed. Engl.* **1989**, *28*, 1065 – 1066; b) Z. R. Qu, H. Zhao, Y. P. Wang, X. S. Wang, Q. Ye, Y. H. Li, R. G. Xiong, B. F. Abrahams, Z. G. Liu, Z. L. Xue, X. Z. You, *Chem. Eur. J.* **2004**, *10*, 53 – 60; c) T. Okubo, R. Kawajiri, T. Mitani, T. Shimoda, *J. Am. Chem. Soc.* **2005**, *127*, 17598 – 17599.

[9] a) O. A. Aktsipetrov, O. V. Braginskii, D. A. Esikov, *Sov. J. Quantum Electron.* **1990**, *20*, 259 – 263; b) T. V. Murzina, R. V. Kapra, T. V. Dolgova, A. A. Fedyanin, O. A. Aktsipetrov, K. Nishimura, H. Uchida, M. Inoue, *Phys. Rev. B* **2004**, *70*, 012407; c) M. Fiebig, D. Fröhlich, B. B. Krichevtsov, R. V. Pisarev, *Phys. Rev. Lett.* **1994**, *73*, 2127 – 2130.

[10] a) W. D. Griebler, D. Babel, *Z. Naturforsch. B* **1982**, *37*, 832 – 837; b) S. Ohkoshi, T. Iyoda, A. Fujishima, A. K. Hashimoto, *Phys. Rev. B* **1997**, *56*, 11642 – 11652.

[11] S. Ohkoshi, K. Hashimoto, *Chem. Phys. Lett.* **1999**, *314*, 210 – 214.

